He-Ne Laser

S. Rager (sr3874)[1]
[1] *PHYSUN3801 Columbia University*
(Dated: 17:01 Sunday 20th October, 2024)

A helium-neon laser was constructed to understand the properties of lasers. Specifically, the transverse and longitudinal modes were observed, its power was measured, and it was compared to a commercial solid-state laser.

AIM

To construct a helium-neon laser, view its transverse and longitudinal modes, compare them to a commercial solid-state lase, and calculate its power.

INTRODUCTION & METHOD

Laser stands for light amplification by stimulated emission of radiation. A laser produces spatially coherent electromagnetic radiation with a narrow spectral width.

For a He-Ne laser, 90% He and 10% Ne are mixed at low pressure within a tube. An electrical current ionizes the gas forming a plasma of helium atoms in metastable states. For these states, one valence electron of helium is excited to the 2s energy level and disallowed from decaying back to the ground level by quantum mechanical selection rules. Since the 2s helium level and the 4s and 5s neon levels are close in energy, collisions between helium and neon atoms increase the probability of a neon electron being excited to the 4s or 5s energy level. When this occurs, the helium electron drops back to the ground state, but there are roughly ten times as many helium atoms as neon atoms, so there are more neon electrons in the 4s and 5s levels than lower excited levels and a population inversion is created.

Once a population inversion is achieved by pumping the system with electrical charge, stimulated emission leads to the neon electrons transitioning to lower energy levels. The most common transition is the $5s \rightarrow 3p$ transition which emits a photon of wavelength $\lambda = 632.8$nm. These emitted photons are then confined using reflecting mirrors. Since each emitted photon has a chance of stimulating the emission of an identical additional photon from a second excited neon atom, carefully aligning the mirrors allows one to increase the effective length of the cavity and produce a powerful beam of coherent radiation. The mirrors allow about 1% transmission of laser radiation. The internal beam is approximately 100 times more powerful than the external beam.

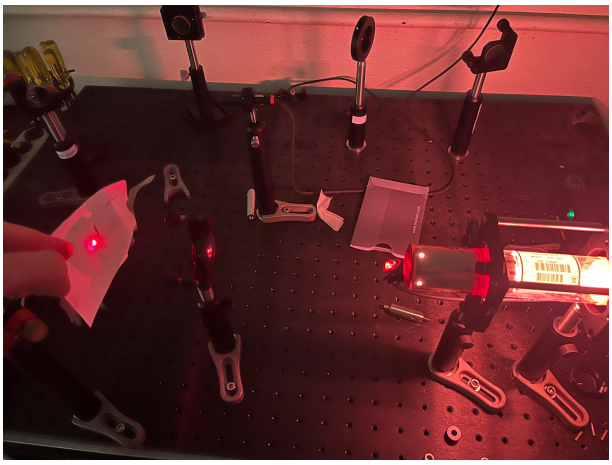

FIG. 1. First Lase

To construct the laser, a voltage was applied to a tube filled with helium and neon as described in the introduction. The tube had a mirror glued in place and the majority of the time spent constructing the laser was devoted to aligning the second mirror to establish the cavity and allow the laser to lase. The height, position, and angle of the mirror was adjusted at the base of its stand while the fine adjustment screws remained neutral. Once a roughly correct position for the mirror was established, the adjustment screws were used to maintain the lasing. When lasing is achieved but then destroyed, the window of the laser flashes red, indicating that the mirror is in roughly the correct position. FIG. 1. shows the first time lasing was achieved.

Transverse modes were produced by using the fine adjustment screws to slightly misalign the mirror and introduce impurities into the cavity. This changed the boundary conditions of the optical resonator. Changing the boundary conditions results in different wave solutions to Maxwell's equations as was observed. Another mirror was then used to throw the beam as far as possible in order to view the transverse modes. For the laser purchased from ThorLabs, a mirror was used to throw the beam as far as possible, and its non-Gaussian transverse mode was viewed; however, no alterations were able to be made to the cavity due to its small size.

Longitudinal modes were observed by coupling the laser beam into a Fabry Perot interferometer using two lasers. Longitudinal modes are caused by the interference of standing waves, hence the use of an interferometer to observe them. The general characterization of a Fabry Perot is that a path difference can be created between reflected and transmitted beams of light for light incident on a set of partially reflective mirrors. This path difference is proportional to the angle of incidence and the separation of the mirrors. A fringe pattern is then formed when the beams are recombined due to interference. Changing the separation distance between the mirrors thus changes the

amount of constructive and destructive interference which also changes the pattern observed.

The Fabry Perot was driven by a traingular waveform at 50Hz from a Wavetek Model 182A function generator connected to channel 1 of the osciloscope. The Fabry Perot was connected to channel 2. The applied voltage linearly translated a spherical mirror via a piezo-electric crystal to scan through the free spectral range of the laser while another spherical mirror remained stationary to form the cavity of the Farby Perot which allowed the light to interfere. FIG. 3. is a schematic of the output of the Fabry Perot. The free spectral range was measured using an oscilloscope connected to the output of the Fabry Perot. The free spectral range was then equated to 8GHz as know from theory to adjust the scale of the oscilloscope. This metric was then used to adjust the full width half maximum measured on the oscilloscope. Finally, the free spectral range was divided by the adjusted full width half maximum to find the finesse of the Fabry Perot interferometer. These calculations were repeated for 5 different cavity lengths of 20±5mm, 40±5mm, 60±5mm, 80±5mm, and 100±5mm. In an attempt to better understand how a Fabry Perot interferometer works, the beam was also coupled into a 100 year old Fabry Perot interferometer that used screws to adjust the length of its cavity rather than a piezo-electric crystal. The coarse adjustment dial did not function because the seal that kept it engaged after it was screwed past a certain point was worn out. The rest of the device did and each thread of the screws corresponded to a movement of a quarter wavelength.

The power of the constructed laser was measured using an multimeter and a biased detector from ThorLabs. The biased detector was placed outside of the laser cavity and a volt measurement was taken. This measurement was then converted into a current using the resistivity of the coaxial cables connecting the detector and the multimeter. The current thus derived was then divided by the quoted responsivity of the detector found in the biased detector user manual[II] to provide a power reading.

RESULTS & ANALYSIS

Transverse Modes

Appendix I shows pictures of the observed transverse modes obtained via the methodology above. They appear blurrier reproduced here than they appeared in the laboratory due to the image processing software on iPhones. FIG. 2 shows a comparison of the Gaussian transverse modes of the constructed helium-neon laser on the left and the non-Gaussian transverse modes of the 635nm Compact Laser Module[III] with USB purchased from ThorLabs.

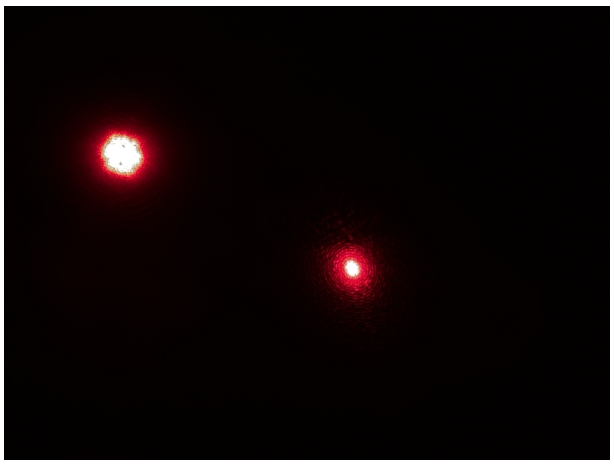

FIG. 2. Comparison of Gaussian and non-Gaussian transverse modes

Longitudinal Modes

Appendix II contains images of the output of the Fabry Perot as viewed on the oscilloscope for cavity lengths of 20±5mm±5, 60±5mm, and 100±5mm which were achieved by changing the position of the mirror originally used to establish lasing. Data collected for cavity lengths of 20±5mm, 40±5mm, 60±5mm, 80±5 mm, and 100±5mm are presented in the table below. Measurements of the free spectral range were taken for each cavity length. A sample calculation goes as follows. Free spectral range (FSR)= peak to peak distance of blue channel on oscilloscope=3.36 ms. Knowing FSR=8GHz implies a Hz to s conversion of $2.38(10^{12})$Hz/s. The measured full width half maximum (FWHM) of the blue channel was 560µs. This converts to $1.33(10^{9})$Hz. Finally,

$$Finesse = \frac{FSR}{FWHM} = \frac{8}{1.33} \approx 6$$

Cavity Length(mm)	20±5	40±5	60±5	80±5	100±5
FSR(ms)$_{\pm 10^{-4}}$	1.564	1.584	2.292	1.68	2.204
FWHM(µs)	356±30	540±20	860±12	410±12	572±12
Finesse	4.4±0.37	2.9±0.11	2.7±0.04	4.1±0.12	3.9±0.08

The finesse quoted in the Fabry Perot manual was a minimum of 150; however, our result makes sense in light of the age of the equipment, the amount of dust in the room, and the myriad of other things affecting the purity of our cavity. Had the finesse of the Fabry Perot been greater, we would have expected to see a frequency structure within each pulse on the oscilloscope and this was not observed, also indicating the poor finesse of the system.

The same methodology for viewing the longitudinal modes of the constructed laser was applied to the purchased laser, but nothing except noise registered on the oscilloscope. To rule out the possibility of misalignment on the part of the experimenters, we coaligned the constructed and commercial lasers' beams before coupling the coaligned beam into the Fabry Perot. FIG. 4 shows the coalignment and the

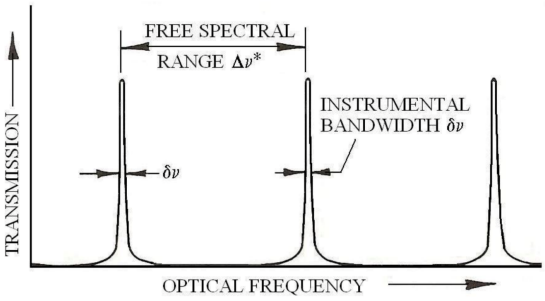

FIG. 3.

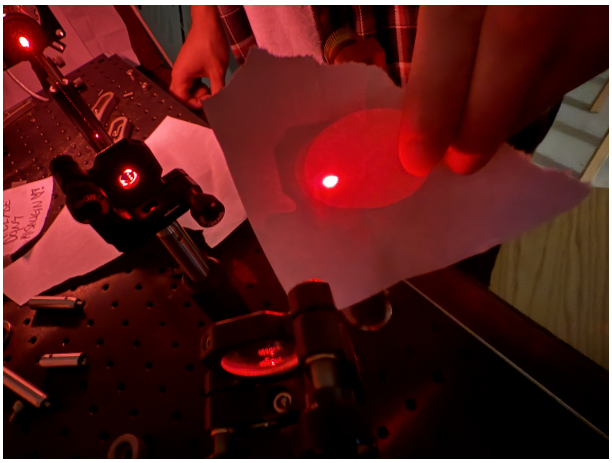

FIG. 4. Coalignment of the constructed and purchased lasers

output of the Fabry Perot for this set up can be viewed in Appendix II. When the He-Ne laser was left on along with the purchased laser, the Fabry Perot output a series of pulses, indicating the alignment of the system. When the He-Ne laser was switched off with the purchased laser remaining on, the Fabry Perot went back to outputing noise. It is further hypothesised by the researchers that the constructed He-Ne laser selects frequencies better than the commercial solid-state laser because it has a greater cavity length. Therefore, it also has a greater free spectral range. Since the instrumental bandwidth is a property of the Fabry Perot, the finesse for the solid-state laser must be less than 6, the greatest finesse measured though the measurement was taken without a corresponding cavity length measurement, and not enough to resolve anything other than noise.

$$FSR_{ss} < FSR_{HN}, 6 = \frac{FSR_{HN}}{FWHM} \Rightarrow \frac{FSR_{ss}}{FWHM} < 6$$

FIG. 5 shows an attempt at viewing circular fringes using the 100 year old mechanical Fabry Perot. Linear fringes were achieved but not photographed. Appendix II also contains an image displaying a similar pattern by removing the back piece of the piezoelectric Fabry Perot and throwing the beam onto the wall instead of measuring it with the osciloscope.

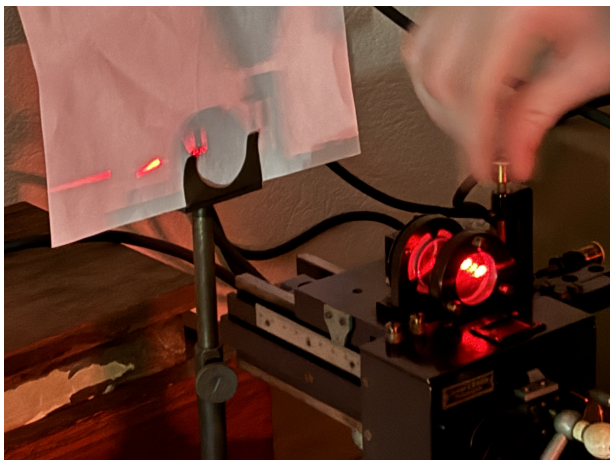

FIG. 5. Attempt to view fringes on 100 year old Fabry Perot Interferometer

Power

Power was calculated as in the methodology. A volt reading of 0.296V was obtained. This was then converted to a current using the 50Ω resistance of the coaxial connecting cable to find I_{out}. In principle a measurement of the dark current should have been taken for the biased detector and subtracted from I_{out}, but the quoted[II] dark current of T_{dark}=0.35nA was negligible and the measurement tools available would not have provided a meaningful measurement.

$$P = \frac{I_{out}}{Responsivity} = \frac{0.296 \pm 0.001 V/50A}{0.325 \pm 0.025 A/W} = 18 \pm 0.288 mW$$

This power rating identifies the constructed laser as a class 3B laser, one class lower than the highest which is class 4. The standard warning for class 3B lasers is that they are capable of burning materials if left incident on them for too long. However, in approximately 16 hours of laboratory nothing was ever burned.

CONCLUSIONS

A He-Ne laser was constructed and its transverse and longitudinal modes observed. The transverse modes were stable in time, remaining unchanged when the system was perturbed such as by jostling the table. It is believed that TEM (3,3) was observed; however, the resolution of the transverse modes decreased with increasing mode number due to the finite length of the room. Compared to the transverse modes, the longitudinal modes were not stable in time and very sensitive to mechanical disturbances. An average finesse of 3.6±0.14 was calculated for the Fabry Perot, essentially two orders of magnitude smaller than the quoted value of 150 from the manual. Finally, the power of the He-Ne laser was measured to be 18±0.288mW.

ACKNOWLEDGEMENTS

Benjamin Graeme Gorman (bgg2112) for his contributions as my lab partner

I. PHYSUN3081 Spring 2020 Intermediate Laboratory Work The HeNe Laser, accessed Sunday 20th October, 2024, <https://www.columbia.edu/∼mm21/exp_files/laser_exp.pdf>.

II. ThorLabs Det36A2 Si Biased Detector User Guide, accessed Sunday 20th October, 2024, <https://www.thorlabs.com/drawings/64902eed6a4039cc-4117B704-CB08-1524-87392EC4744CC3ED/DET36A2-Manual.pdf>.

III. ThorLabs PL202 Spec Sheet, accessed Sunday 20th October, 2024, <https://www.thorlabs.com/drawings/4783ea505cdcf716-A95D35A9-F346-95C8-29C2B611B388E810/PL202-SpecSheet.pdf>.

He-Ne Laser Appendix I (Transverse Modes)

S. Rager (sr3874)

(0,0)

(1,1)

(0,1)

(1,2)

(0,2)

(2,2)

Higher Order Mode Believed to be (3,3)

Link to Download Transverse Mode Video from Google Drive: https://drive.google.com/file/d/1KCTkuLVb232WdB5JmI4ttRbPgrJQfm_x/view?usp=drive_link

Link to Download Transverse Mode Stability Video from Google Drive: https://drive.google.com/file/d/11cG6BKNMQn4LaYBZJI_r4TzHaPiOHO6S/view?usp=drive_link

He-Ne Laser Appendix II (Longitudinal Modes)
S. Rager (sr3874)

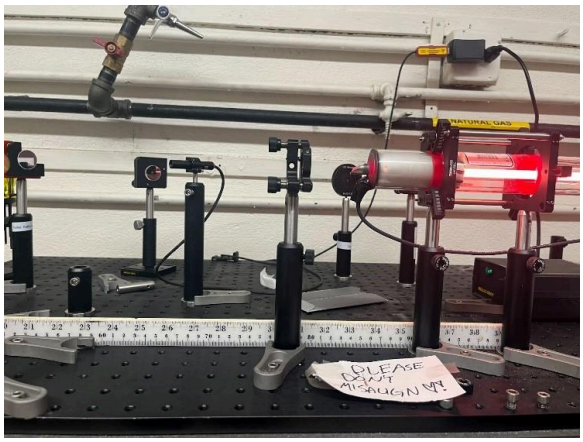

Cavity Length:~20mm

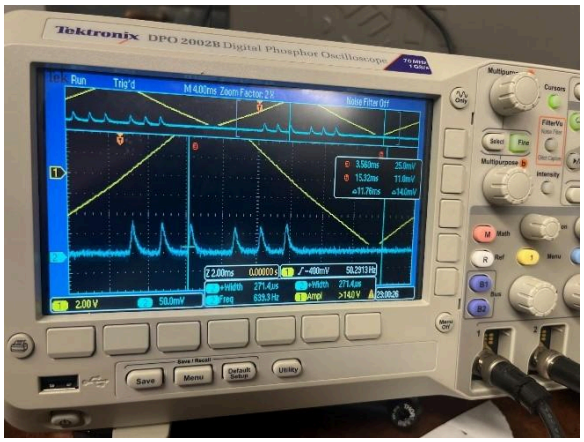

Fabry Perot Output (60mm)

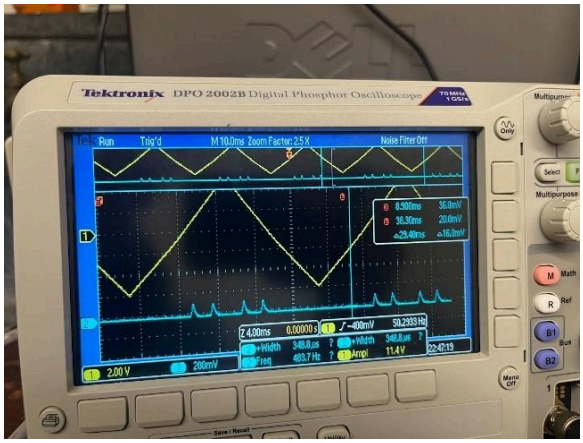

Fabry Perot Output (20mm)

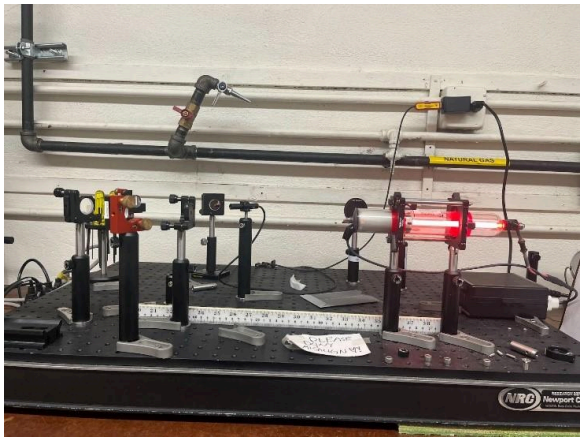

Cavity Length:~ 100mm

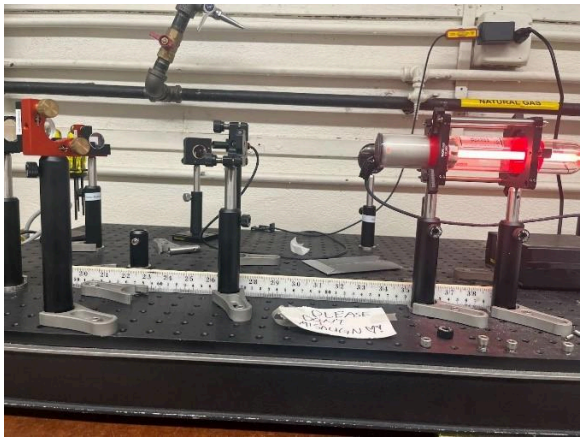

Cavity Length:~60mm

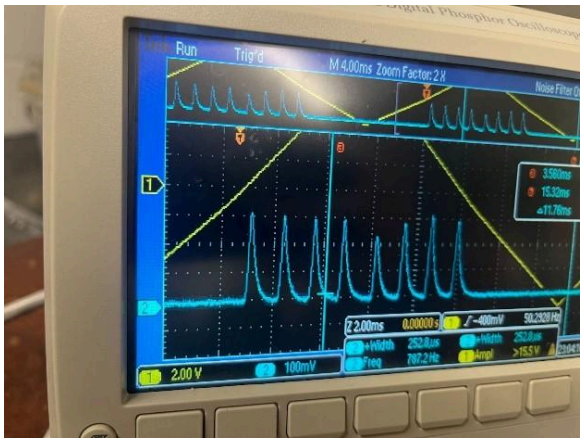

Fabry Perot (100mm)

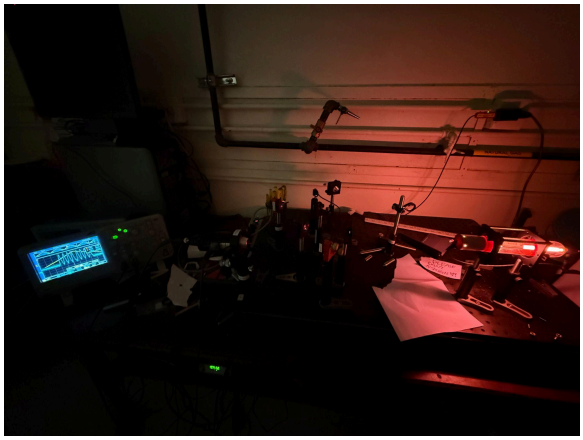

Coaligned Beams with Fabry Perot Output

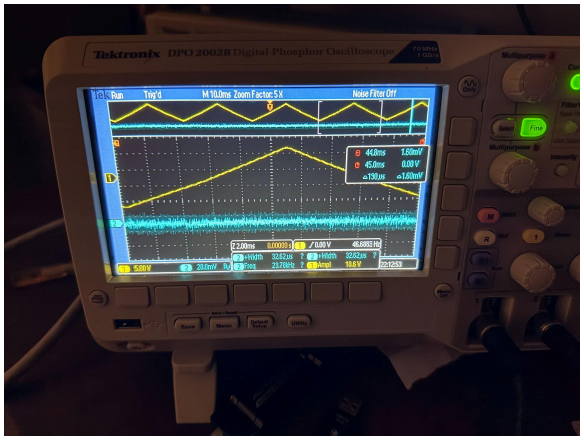

Fabry Perot Output Commercial Laser

Fabry Perot Output for Both Beams at Once

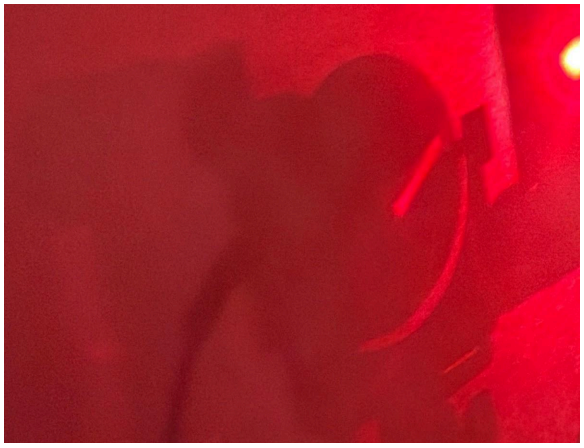

Piezo-Eelctric Fabry Perot End Piece Removed

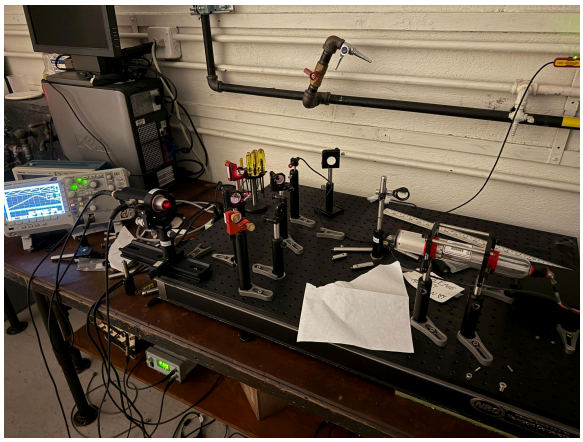

Coaligned He-Ne Laser Turned Off

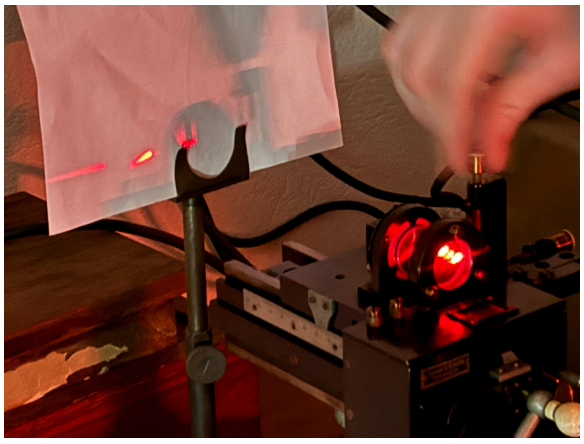

Mechanical Fabry Perot
Link to Download Longitudinal Mode Video from Google Drive:
https://drive.google.com/file/d/1IPsoZHeLnmK7KoNGhG2lbAuFybRypngw/view?usp=drive_link